Icarus 229 (2014) 221–235

Contents lists available at ScienceDirect

Icarus

journal homepage: www.elsevier.com/locate/icarus

Hollows on Mercury: Materials and mechanisms involved in their formation ☆

Rebecca J. Thomas [a,*], David A. Rothery [a], Susan J. Conway [a], Mahesh Anand [a,b]

[a] Department of Physical Sciences, The Open University, Walton Hall, Milton Keynes MK7 6AA, UK
[b] Department of Earth Sciences, Natural History Museum, Cromwell Road, London SW7 5BD, UK

ARTICLE INFO

Article history:
Received 30 May 2013
Revised 17 October 2013
Accepted 13 November 2013
Available online 21 November 2013

Keywords:
Mercury, surface
Geological processes
Impact processes

ABSTRACT

Recent images of the surface of Mercury have revealed an unusual and intriguing landform: sub-kilometre scale, shallow, flat-floored, steep-sided rimless depressions typically surrounded by bright deposits and generally occurring in impact craters. These 'hollows' appear to form by the loss of a moderately-volatile substance from the planet's surface and their fresh morphology and lack of superposed craters suggest that this process has continued until relatively recently (and may be on-going). Hypotheses to explain the volatile-loss have included sublimation and space weathering, and it has been suggested that hollow-forming volatiles are endogenic and are exposed at the surface during impact cratering. However, detailed verification of these hypotheses has hitherto been lacking.

In this study, we have conducted a comprehensive survey of all MESSENGER images obtained up to the end of its fourth solar day in orbit in order to identify hollowed areas. We have studied how their location relates to both exogenic processes (insolation, impact cratering, and solar wind) and endogenic processes (explosive volcanism and flood lavas) on local and regional scales. We find that there is a weak correlation between hollow formation and insolation intensity, suggesting formation may occur by an insolation-related process such as sublimation. The vast majority of hollow formation is in localised or regional low-reflectance material within impact craters, suggesting that this low-reflectance material is a volatile-bearing unit present below the surface that becomes exposed as a result of impacts. In many cases hollow occurrence is consistent with formation in volatile-bearing material exhumed and exposed during crater formation, while in other cases volatiles may have accessed the surface later through re-exposure and possibly in association with explosive volcanism. Hollows occur at the surface of thick flood lavas only where a lower-reflectance substrate has been exhumed from beneath them, indicating that this form of flood volcanism on Mercury lacks significant concentrations of hollow-forming volatiles.

© 2013 The Authors. Published by Elsevier Inc. All rights reserved.

1. Introduction

The presence of morphologically fresh depressions on the surface of Mercury has been one of the most surprising discoveries of the MESSENGER (MErcury Surface, Space ENvironment, GEochemistry, and Ranging) spacecraft. Though areas of hollows had been imaged at low resolution by the Mariner 10 spacecraft in the 1970s, they appeared only as high-reflectance, spectrally relatively blue patches on the floors of impact craters (BCFDs – Bright Crater Floor Deposits) (Dzurisin, 1977; Robinson et al., 2008; Blewett et al., 2009). When MESSENGER went into orbit in 2011 and obtained higher-resolution images, these were revealed to be clusters of irregular rimless depressions with flat floors and steep walls (Fig. 1). These were dubbed 'hollows' to distinguish them from deeper 'pits' with sloping floors, which are proposed to form through magmatic processes (Gillis-Davis et al., 2009; Kerber et al., 2011). They range from individual hollows tens of meters across to clusters of hollows tens of kilometres across (Blewett et al., 2011) and shadow measurements indicate a consistent depth within a particular host crater in the range of tens of meters (Blewett et al., 2011; Vaughan et al., 2012). Though their consistent depths make them flat-floored overall, lumps of material do occur on hollow floors that may be degraded remnants of the original surface (Blewett et al., 2011). The bright deposits that gave BCFDs their name are revealed from orbit to occur both on hollow floors and as surrounding haloes.

Hollows appear morphologically fresh and lack superposed impact craters. This implies a young age and suggests hollow formation may be an on-going process (Blewett et al., 2011). If so, it will be important to distinguish whether it is a gradual, continual process or a more rapid, episodic process.

☆ This is an open-access article distributed under the terms of the Creative Commons Attribution License, which permits unrestricted use, distribution, and reproduction in any medium, provided the original author and source are credited.

* Corresponding author.
E-mail address: rebecca.thomas@open.ac.uk (R.J. Thomas).

0019-1035/$ - see front matter © 2013 The Authors. Published by Elsevier Inc. All rights reserved.
http://dx.doi.org/10.1016/j.icarus.2013.11.018

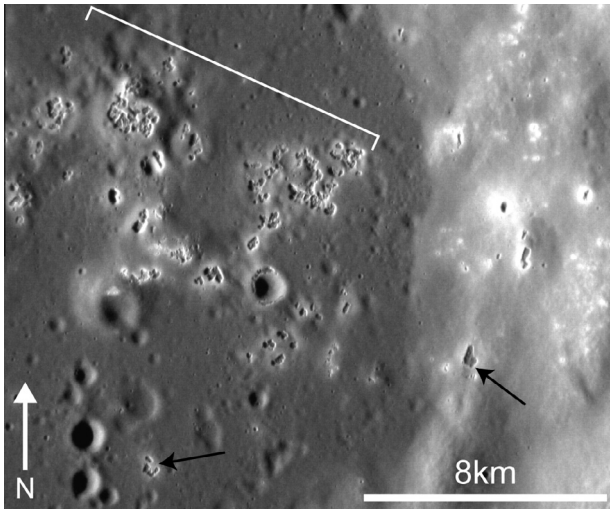


Fig. 1. Irregular, rimless hollows on the floor and terraced wall of an unnamed impact crater at 46.4°N, 318.7°E. Black arrows indicate individual hollows, white bracket indicates a cluster (MESSENGER image ID 2760274).

The flat-floored, closed morphology of hollows and the lack of associated outflow features suggest that they form by the preferential loss of a volatile component from the surface without melting. The nature of this material is not known: sulphides or chlorides are possible candidates (Vaughan et al., 2012; Blewett et al., 2013; Helbert et al., 2013) but the current resolution of surface elemental compositional data (Goldsten et al., 2007; Hawkins et al., 2007; Schlemm et al., 2007; Nittler et al., 2011; Peplowski et al., 2011; Evans et al., 2012; Weider et al., 2012) is not sufficient to verify this at the scale of hollows.

Several possible release mechanisms for this volatile substance have been suggested (Blewett et al., 2011). The feasibility of these processes is dependent on the nature of the substance lost and the timescale of hollow formation. In light of the high daytime surface temperatures at Mercury and the morphological similarity between hollows and the 'Swiss cheese terrain' of Mars (Thomas et al., 2000), sublimation is a strong candidate. However, various forms of space weathering are believed to occur at Mercury, and these may be important release mechanisms if they are relatively intense in the material where hollows form. Along with thermal desorption (Madey et al., 1998), photon stimulated desorption (PSD) releases alkalis from the surface and may be the most efficient form of space weathering supplying these elements to the exosphere (Cheng et al., 1987; Mura et al., 2009). On a shorter timescale and at particular localities, physical (Killen et al., 2004) and perhaps chemical (Potter, 1995) sputtering by the solar wind may also be important, with the intensity of these processes depending on the time-variable interaction between the solar wind and the planet's magnetic field. Micrometeorite impact vaporisation also releases material from the surface, and unlike the processes mentioned above, penetrates beyond the layer of atoms at the extreme surface (Killen et al., 2007). The rate of hollow formation may however be too fast for this to apply (Blewett et al., 2011).

Hollows usually occur in material with a low reflectance relative to the Hermean average. In some cases this is a regional deposit equating to the LRM (low-reflectance material) spectral unit that has been mapped over large areas of the planetary surface (Denevi et al., 2009), in others it is a localised deposit, and in a few cases it is a small 'dark spot' with even lower reflectance than LRM (Xiao et al., 2013). Low-reflectance material may therefore be the volatile-bearing unit that degrades to form hollows. The question arises of how the volatile component in this material has been able to access the surface recently enough to form fresh landforms despite considerable evidence for global contraction (Strom et al., 1975; Watters et al., 2009): this stress state would tend to hinder migration of material through the crust. The correlation of hollow formation with impact craters strongly suggests that impacts are involved in bringing the hollow-forming volatiles to the surface. It has been suggested that this may occur through exposure in crater walls, floors and ejecta and exhumation in peak structures (Blewett et al., 2013), or through differentiation of impact melt (Vaughan et al., 2012).

A deeper understanding of the distribution and mode of occurrence of hollows is of great interest because of the probable relationship between hollows and volatile percentage in Mercury's crust, now understood to be higher than previously thought (Kerber et al., 2009, 2011; Nittler et al., 2011; Peplowski et al., 2011). We have therefore conducted a full survey of MESSENGER images of Mercury's surface. This comprehensive survey has allowed identification of many areas of hollow formation not previously recognised, building on the global inventory published by Blewett et al. (2013). We have recorded the extent, location and associations of the observed hollow clusters, and examined latitudinal and longitudinal variations in their areal extent. We consider how their occurrence and extent may be controlled by external factors such as insolation and ion sputtering or endogenic processes such as the formation of pyroclastic pits or surficial coverage by thick volcanic plains. On a local scale, we have examined the slope aspects in locations where hollows occur on slopes, in order to test whether there is a correlation with insolation intensity, and have studied the local settings of hollow formation to evaluate possible exposure mechanisms for hollow-forming volatiles.

2. Methods

2.1. MESSENGER imagery

We examined images taken by MESSENGER's Mercury Dual Imaging System (MDIS) (Hawkins et al., 2007, 2009) up to the end of MESSENGER's fourth solar day in orbit around Mercury (product creation times up to March 17, 2013). Monochrome images were used to identify hollows and study them in detail, and lower resolution colour composites were used to determine the spectral character of their associated deposits and substrates.

2.1.1. Monochrome images

We examined all MESSENGER monochrome images with resolutions of less than 180 m/px, excluding images at lower resolutions because they do not reveal the irregular margins, flat-floors and rimlessness that distinguish hollows from small impact craters. These images were obtained by the 1.5° field-of-view Narrow Angle Camera (NAC) and the 748.7 nm filter in the 10.5° field-of-view Wide Angle Camera (WAC) of MDIS. The highest-resolution images used were 7.7 m/px and the average resolution of those available was 106 m/px.

We applied radiometric and photometric correction to all images using the ISIS3 image processing package of the USGS. We then overlaid these onto the 250 m/px global monochrome mosaic version 9 produced by the MESSENGER team (released by NASA's Planetary Data System on 8 March 2013) and digitised features on this global mosaic.

2.1.2. Colour images

To characterise the spectral type of local and regional substrates, we examined colour composites created by combining data from three of the twelve spectral filters in the WAC. All major substrates on Mercury have red-sloped reflectance spectra (Denevi et al., 2009), but the steepness of this slope varies, allowing some

to be classified as red or blue relative to the Hermean average. By combining reflectance at 996 nm, 749 nm and 433 nm in the red, green and blue bands, we were able to see these variations and attribute substrates to the spectral types established by Denevi et al. (2009), which are believed to indicate real compositional and geological differences between surface units.

All images at a resolution of less than 1000 m/px were examined, as was the 1000 m/px global colour mosaic version 3 produced by the MESSENGER team (released by NASA's Planetary Data System on 8 March 2013). The highest-resolution composite created was 64 m/px and the average resolution was 455 m/px.

2.2. Data collected

2.2.1. Hollows and pits

Data on all non-impact-related depressions visible in the images were gathered in order to ensure that a distinction was made between hollows and pits with a probable magmatic (Gillis-Davis et al., 2009) or pyroclastic (Kerber et al., 2011) origin and to make spatial comparisons between this activity and hollow formation. Impact-related craters were distinguished from pits and hollows on the basis of their circular shape, raised rims and the characteristic geometry of their ejecta blankets.

The steepness of a depression's margins and the spectral signature of its associated deposits were used to distinguish between hollows and pits: hollows have steep margins leading to flat floors and bluer deposits while pits have gentler slopes, are deeper, and any surrounding deposits are redder (Table 1). We identified a third previously unidentified type of depression that is intermediate in character between pits and hollows: areas of pitted ground floored by relatively red deposits. These either lack defined margins or have steep margins that appear less crisp than those of hollows. Where they have defined margins, they are intermediate in depth between hollows and pits. The presence of relatively red deposits in these regions, the lack of relatively blue deposits and their smoother morphology suggests that these are not hollows. The similarity of the spectral character of their deposits to those of pits, which are suggested to be formed by explosive volcanism (Kerber et al., 2011), may indicate a volcanic origin.

For each depression, we gathered data on its geographical location, area, association with tectonic structures such as thrust faults, the spectral type of the local and regional substrate, and the type of material hosting it. We identified the spectral type of the regional substrate by reference to global mapping by Denevi et al. (2009, 2013) and our own observations of colour composite images, distinguishing between regional low-reflectance material (LRM), intermediate terrain (IT), high-reflectance plains (HRP) and low-reflectance blue plains (LBP). On a local scale, we noted the presence of relatively red material, bright ejecta deposits and localised low-reflectance material. To record the host material we distinguished between the walls, peak structure, ejecta blanket and smooth or rough floor of craters, and smooth and rough non-crater surfaces.

We grouped hollows together on the basis of occurrence within a particular host crater or location within 50 km of each other where they lie outside craters. We calculated the areal extent of hollows within each group by mapping them individually and obtaining the spherical area (area of a polygon without the distortion caused by map projection) using the Graphics and Shapes tool for ArcGIS (Jenness, 2011).

As several of the proposed formation mechanisms for hollows are controlled by insolation, we investigated the possibility of preferential hollow formation on sun-facing slopes. We recorded the aspect of the slope where hollows within a group occurred on slopes of a particular orientation where that observed orientation could not be explained by compositional differences or differences in viewing conditions for nearby slopes at other orientations. This aspect was taken to be the bearing of a line normal to the horizontal alignment of hollows along the surface of the slope. This was drawn by eye and rounded to the nearest 5°, as no digital terrain model of adequate resolution was available.

In order to calculate the depths of hollows, we measured shadows at the margins of hollows in cases where high resolution (<110 m/px) images were available. A precision of half a pixel was used to estimate the error. Where multiple images were available of the same hollow, we used the image with the highest resolution and lowest emission angle (angle off nadir) to minimise error. We also avoided measuring shadows falling on steep slopes.

Because pits are generally larger-scale features than hollows and since we wanted to investigate whether hollows occur in association with pits, we noted whether the resolution of the available images of pits would allow identification of hollows, if present.

2.2.2. Impact craters

Where hollows occur in association with an impact crater we noted the crater diameter as a proxy for depth of excavation. This was obtained from the Herrick et al. (2011) global crater database or measured on a sinusoidal projection of the crater if it was not within that database. We also noted the crater's degree of degradation as a proxy for age using the scheme of Barnouin et al. (2012). Degradation classes range from 1 to 5 (oldest to youngest) and are defined on the basis of characteristics such as the preservation of the ejecta blanket, modification of terraces and amount of superposed impact craters. Any crater ages mentioned in this work are based on this scale.

3. Results

We found 445 groups of hollows, covering 57,400 km^2, which amounts to 0.08% of the surface area imaged at better than 180 m/px (locations indicated in Supplementary material). These ranged in areal extent from 0.07 km^2 to 6771 km^2, with a mean of 129 km^2 (standard deviation = 475). 140 of these groups were at locations previously catalogued by Blewett et al. (2013). We also identified 173 groups of pits and 24 areas of spectrally red pitted ground (Fig. 2).

Table 1
Characteristics distinguishing pits, hollows and spectrally red pitted ground.

Characteristic	Hollows	Pits	Spectrally red pitted ground
Wall slope	Steep	Shallow	Lacking or steep
Floor slope	Flat, though lumps of material may occur	Sloping	Roughly horizontal but uneven
Surrounding deposits (when present)	High-reflectance, relatively blue	High-reflectance, relatively red	High-reflectance, relatively red
Depth	Tens of meters	Can be 1 km or more deep (Rothery et al., 2014; Gillis-Davis et al., 2009)	Tens of meters

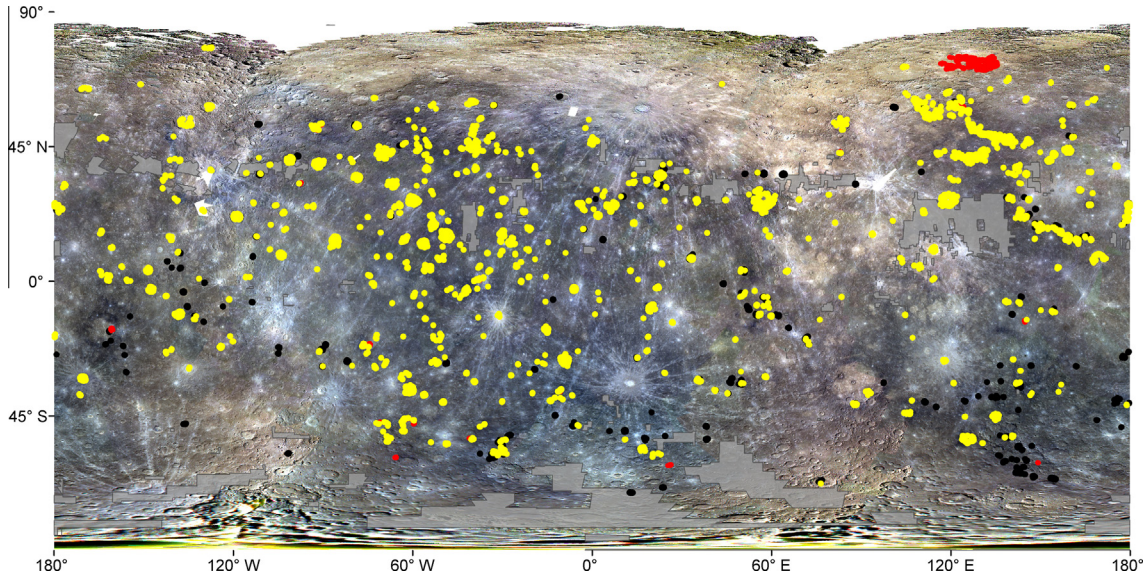


Fig. 2. Global occurrence of hollows, pits and spectrally red pitted ground. Yellow: hollows; black: pits; red: spectrally red pitted ground; grey: area not imaged at <180 m/px. (Base mosaic: MESSENGER global colour v3.) (For interpretation of the references to colour in this figure legend, the reader is referred to the web version of this article.)

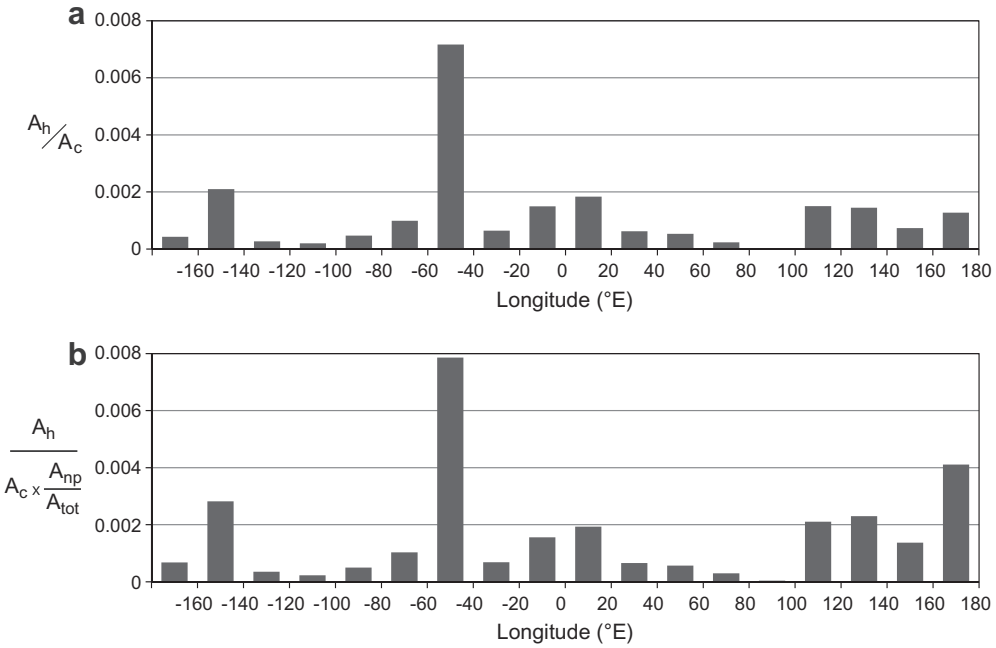


Fig. 3. Variation in the areal extent of hollows (A_h) by longitude bin in the region 30°S to 30°N, normalised to (a) area imaged at <180 m/px (A_c), and (b) $A_c \times$ the fraction of the surface that is not smooth plains (A_{np}/A_{tot}).

3.1. Global variations in the areal extent of hollows

Hollows occur globally, but are rare in the high reflectance plains at high northern latitudes and within basins such as Caloris (160°E, 32°N) and Rembrandt (88°E, −33°N). There is good image coverage in these regions so this absence is not a product of observational bias. Though much of the interior of Caloris lacks hollows, hollows do occur within younger impact craters in its fill. Hollows also occur at its rim, often in association with pits of probable pyroclastic origin, and in two sublinear regions outside its northwest rim.

Though hollows are not observed at high southern latitudes, this could be largely attributable to observational bias: MESSENGER's highly elliptical orbit, with an initial periapsis altitude of 200 km at ~60°N and an apoapsis altitude of 15,200 km (Hawkins et al., 2007), means this area is imaged at much lower resolutions than areas further north.

It has been suggested that hollow formation is controlled by insolation and that hollows rarely occur on smooth plains substrates (Blewett et al., 2013). In order to assess these hypotheses with our global dataset, we investigated whether there is a correlation between longitudinal and latitudinal variations in the areal extent of hollows and in the intensity of insolation and the areal extent of non-plains substrates.

3.1.1. Longitudinal variation

The elliptical orbit of Mercury leads to a variation in mean insolation along the equator: two 'hot poles' (0°E and 180°E) are under

the Sun at perihelion and experience mean temperatures estimated to be 100 K higher than those of two 'cold poles' (−90°E and 90°E), under the Sun at aphelion (Melosh and McKinnon, 1988). To investigate the relationship between hollow occurrence and this longitudinal variation, we calculated the total areal extent of hollows in 20° bins in a 30°S to 30°N equatorial strip, normalising the hollowed area to the area that is imaged at <180 m/px (Fig. 3a). This region has the virtue of being imaged at high resolution and low to moderate solar incidence angles, which are favourable observation conditions for hollows. We found that the areal extent of hollows is low near the 'cold poles', as expected if the intensity of insolation controls their occurrence. The fraction of the surface hollowed between the −40°E to −20°E bin and the 60°E to 80°E bin peaks at the 'hot pole' at 0°E, but a similar pattern of increase is not seen around the other 'hot pole' at 180°E.

However, plains associated with the Caloris basin occupy a large part of the equatorial strip from 150°E to 180°E. To test whether the presence of these plains modifies the pattern of hollow occurrence, we normalised the areal extent of hollows to the fraction of non-plains in each bin, in effect removing the influence of this parameter from the data (Fig. 3b). We then saw a stronger correlation between the extent of hollows and the intensity of mean insolation, indicating that intensity of insolation controls hollow occurrence but is not a sufficient condition for their formation on all substrates.

The large areal extent of hollows in the −60 to −40°E region is a clear anomaly, neither accounted for by the variation in mean insolation nor by the presence or absence of smooth plains.

3.1.2. Latitudinal variation

The fraction of the surface area imaged at <180 m/px that is hollowed varies widely at different latitudes (Fig. 4a). This is in major part attributable to observational bias: this fraction is highest at low and mid-northern latitudes where MESSENGER is closest to the planet and lowest at high southern latitudes where it is furthest away. At very high latitudes, high solar incidence angles (Chabot et al., 2013) also preclude identification of hollows where they occur in craters because large parts of crater interiors are in shadow.

The lack of hollows at high northern latitudes is likely to be further controlled by the presence of a smooth plains substrate here. Normalising to the fraction of non-plains does not entirely remove the disparity between hollow occurrence at low and high northern latitudes (Fig. 4b), but as non-plains areas near the pole are imaged only with high solar incidence angles, it is possible that the remaining disparity is due to observational bias.

The areal extent of hollows at low southern latitudes (−30°N to 0°N) is significantly lower than at low northern latitudes (0–30°N), and this contrast is not removed by normalising to the fraction of non-plains (Fig. 4b). This suggests a further factor discouraging hollowing at low southern latitudes or promoting it at low northern latitudes.

3.2. Preferred slope aspect

It has been suggested that hollows preferentially form on sun-facing slopes and that this is evidence that their formation is linked to solar heating (Blewett et al., 2013). We found some evidence in support of this phenomenon. A preferred aspect was found in only 8% of the groups of hollows observed, but in these cases there was a good correlation to the sun-facing slope (Fig. 5). The small percentage of cases in which a preferred aspect was observed is partly attributable to the fact that only the sun-facing slope is illuminated in many of the available images of hollows at mid- to high latitudes, and in such cases preferential hollow formation on that slope was not recorded because lighting conditions were not good enough to rule out hollow formation on the opposing slope. However, most hollows are found on flat surfaces or on slopes of opposing aspects within a group so we do not find that preferential

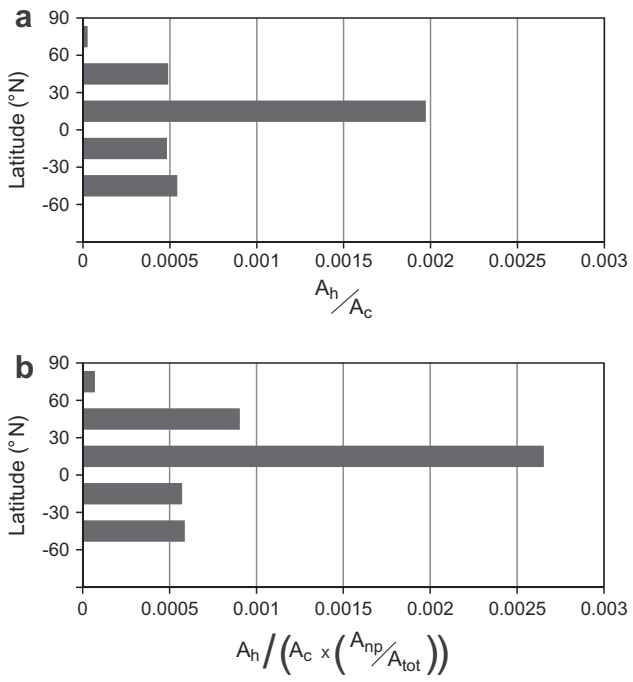


Fig. 4. Latitudinal variations in areal extent of hollows (A_h), normalised to (a) the area imaged at <180 m/px (A_c) and (b) $A_c \times$ the fraction of the surface that is non-plains (A_{np}/A_{tot}) within each latitude bin. Hollow extent varies broadly with image quality, though observational bias does not explain the small extent of hollowing in the 30°S to 0°N bin.

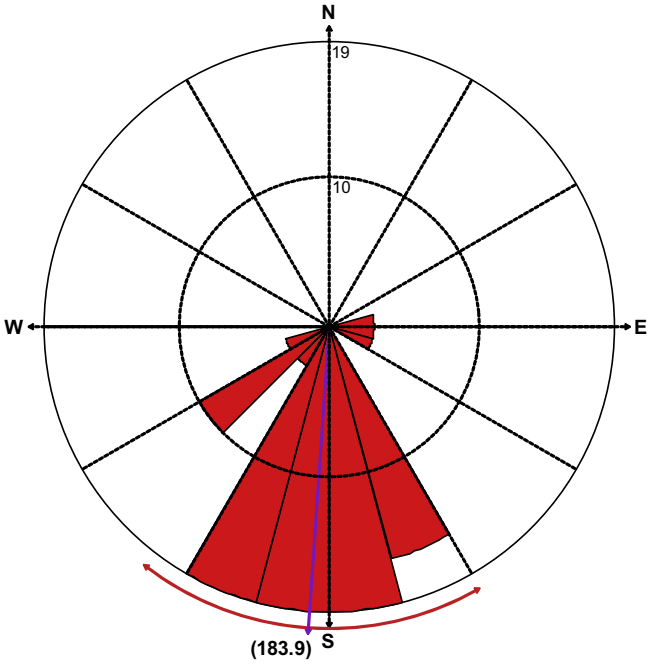


Fig. 5. Aspects of slopes on which hollows preferentially form in the northern hemisphere ($N = 31$), showing a correlation with the sun-facing slope. Purple line indicates the mean, red circumferential line shows one standard deviation. Radial axis: percentage of the population of hollow groups with a preferred aspect within the northern hemisphere. (For interpretation of the references to colour in this figure legend, the reader is referred to the web version of this article.)

formation on sun-facing slopes is a common characteristic of hollows.

3.3. Hollow depth

We calculated a mean depth for hollows of 47 m (standard deviation 21) on the basis of 108 shadow measurements within 27 hollow clusters. Depths ranged from 5 ± 0.75 m to 98 ± 19.5 m. These results are consistent with but more extensive and representative than previous studies showing a hollow depth of ~30 m in Kertesz crater (Vaughan et al., 2012) and 44 m in Raditladi basin (Blewett et al., 2011).

Because of the limited resolution of available images, there is a large error in depth values and it is not possible to identify significant depth variations between different substrates (e.g. peak ring vs. crater floor) or craters of different ages.

3.4. Geological settings

The majority of hollows occur in clusters within impact craters and upon their proximal ejecta, as discussed by Blewett et al. (2013). However, our detailed survey also revealed two large areas of more distributed hollow formation lacking a close relationship with specific craters, and some association with pyroclastic pits in non-crater settings.

3.4.1. Association with impact craters

3.4.1.1. Observations. Hollows occur on a variety of crater surfaces. In simple craters, they commonly occur in a band on the inside rim of the crater (Fig. 6a). In complex craters, they occur on the walls, central structures and smooth floor fill (Fig. 6b) and occasionally on the ejecta blanket. Hollows are commonly clustered, either loosely with small (<5 km) expanses of non-hollowed surface between individual hollows (Fig. 1) or more tightly, as in Fig. 6b, where they form a continuous hollowed area. At the rim of the Caloris basin, many small groups of hollows occur on peaks in the rim material and associated with probable pyroclastic pits.

Where hollows occur on crater fill, they often cluster around the central structures or near the walls (Fig. 6c). In old, degraded craters, they commonly occur on the high inner walls of smaller impacts into the crater or in the hanging walls of crater-crossing thrust faults (Fig. 6d).

3.4.1.2. Statistical correlation. Hollows occur within impact craters and their proximal ejecta in 84.5% of cases, and make up 97.5% of the total global hollowed area. Hollows are therefore strongly associated with craters.

If hollow-forming material is brought to the surface at the time of crater formation, then depending on the duration over which hollows (once formed) remain visible, a correlation could be expected between the age of the crater and the areal extent of

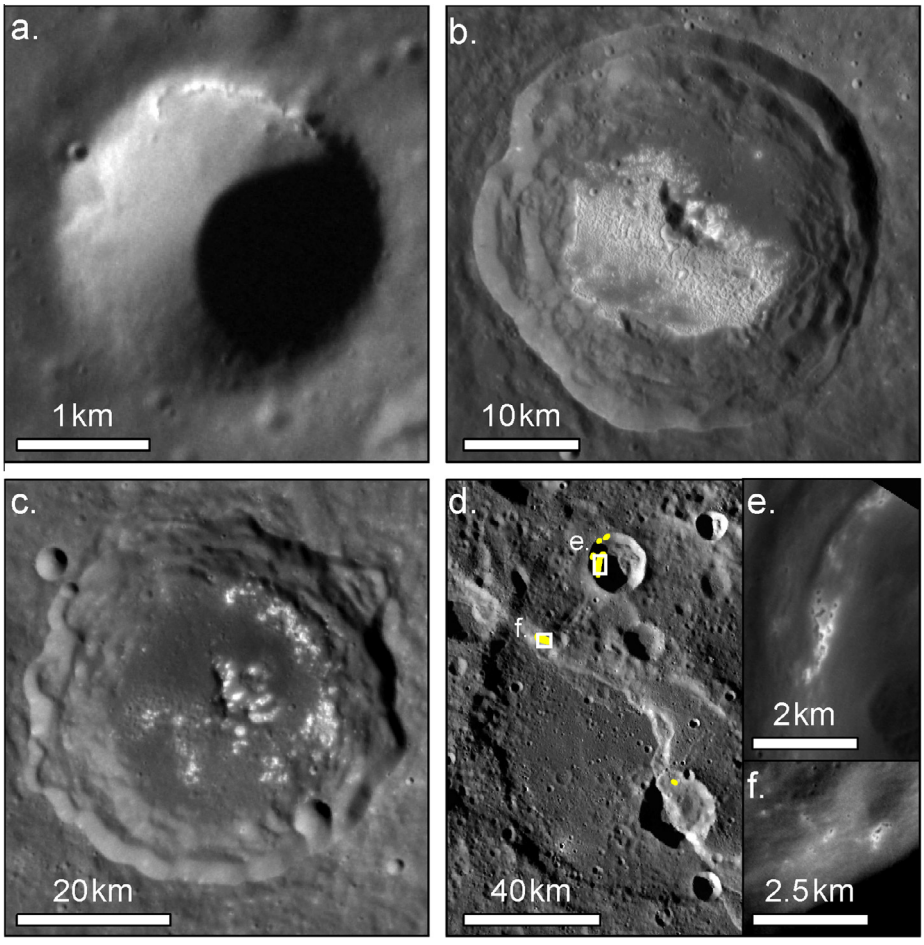


Fig. 6. Typical locations of hollows within impact craters: (a) in a curvilinear band at inner rim of a simple crater (−58.6°E, 57.4°N, EN0238696485M); (b) hollowing across a large part of the floor and peak structure of Hopper crater (Mansurian age, −55.8°E, −12.5°N, EN0223616383M); (c) clustered in the area abutting the crater wall of Nampeyo crater (Mansurian age, −49.9°E, −40.3°N, EN0253678867M); (d) in a young impact into and on a thrust crossing the old, degraded Duccio crater (hollowed areas outlined in yellow) (Tolstojan age, −52.3°E, 58.2°N, MESSENGER global monochrome mosaic); (e) close-up of hollows in a younger impact crater (EN0223658124M); (f) close-up of hollows on a thrust (EN0223614937M). North is towards the top of each image. (For interpretation of the references to colour in this figure legend, the reader is referred to the web version of this article.)

hollowing. We therefore plotted the average extent of hollowing as a percentage of the crater's floor area (πr^2 where r = crater radius) in craters of each degradation state (Fig. 7), using degradation state as a proxy for age (Barnouin et al., 2012). We divided the data into crater diameter bins to allow for the possibility that a similar degradation state may occur in a shorter period for smaller craters than larger craters. We found no clear increase in the percentage of the crater area hollowed in older craters. In fact the average percentage hollowed is somewhat lower in older craters than younger craters (note the logarithmic vertical scale), though it can range up to 5.5% even in very old craters (degradation class 1, signifying a Pre-Tolstojan age). Because slope processes and burial by regolith can potentially obscure the characteristic morphology of hollows (in particular their steep, sharp margins), hollows seen clearly now can be assumed either to be still forming or to have ceased forming in the relatively recent past.

3.4.2. Hollows outside craters

Hollows outside craters make up loose groupings rather than clusters, and in most cases (excluding those discussed below) the extent of hollowing within each group is small, averaging 15.2 km^2 (standard deviation = 38.0). This compares to a mean area of 148.6 km^2 (standard deviation = 514.0) for hollow groups within and in the proximal ejecta of craters. Hollows outside craters usually occur on hummocky surfaces or in a linear pattern cross-cutting geological units, suggesting they formed in distal ejecta (Fig. 8). Some occur around pits with surrounding relatively spectrally red deposits, as reported below (Section 3.5).

The detailed examination undertaken by this study has revealed for the first time two dispersed groupings of hollows covering large areas (136,000 km^2 and 52,000 km^2) roughly radial to the Caloris basin rim and extending to the west and northwest (Fig. 9a). In the western grouping, hollows with an areal extent totalling ~150 km^2 occur on the partially-preserved, heavily-cratered raised rims of old craters that are floored by smooth plains (Fig. 9b). The hollows do not appear to be particularly associated with any one crater but occur wherever this rougher, higher elevation substrate occurs. This substrate can be classified as low-reflectance material (LRM), whereas the crater fills are high reflectance plains (HRP). Hollows in the northwest grouping have an areal extent totalling ~498 km^2. The eastern part of this grouping lies in and around a wide graben outside the northwest rim of the Caloris basin, which may have been carved by ejecta during the Caloris impact event (Fassett et al., 2009). From this area towards the west, hollows occur on the circum-Caloris low-reflectance blue plains (LBP) at the margins of a curvilinear unit of high reflectance material that appears contiguous with a region featuring several broad channels, possibly lava channels (Byrne et al., 2013) near the margins of

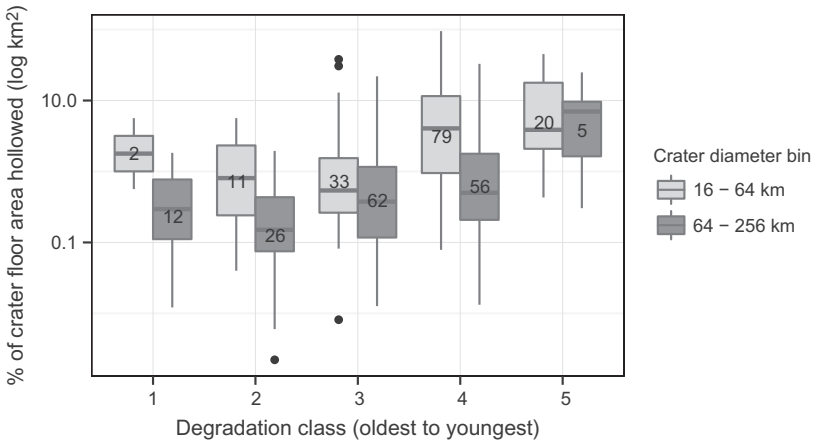


Fig. 7. Spread in area of hollows as a percentage of the calculated crater floor area against the degradation state of the host crater. Bottom and top of boxes indicate the first and third quartiles, band inside each box indicates the median, numbers indicate number of observations and are vertically centred to the mean; lines above and below boxes extend to the most extreme data point where it is no more than 1.5 times the interquartile range; dots indicate outliers.

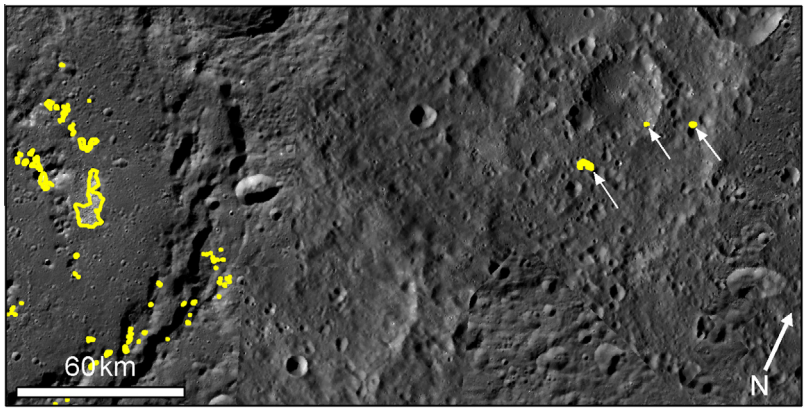


Fig. 8. Hollows of small areal extent (indicated by white arrows) occur approximately radial to a Mansurian-aged unnamed complex crater with hollows on its peak ring, floor and terraces (all hollows outlined in yellow). This association suggests they formed in distal ejecta from the crater. (Figure centred at −65.0°E, 44.8°N, image: excerpt from global monochrome mosaic.) (For interpretation of the references to colour in this figure legend, the reader is referred to the web version of this article.)

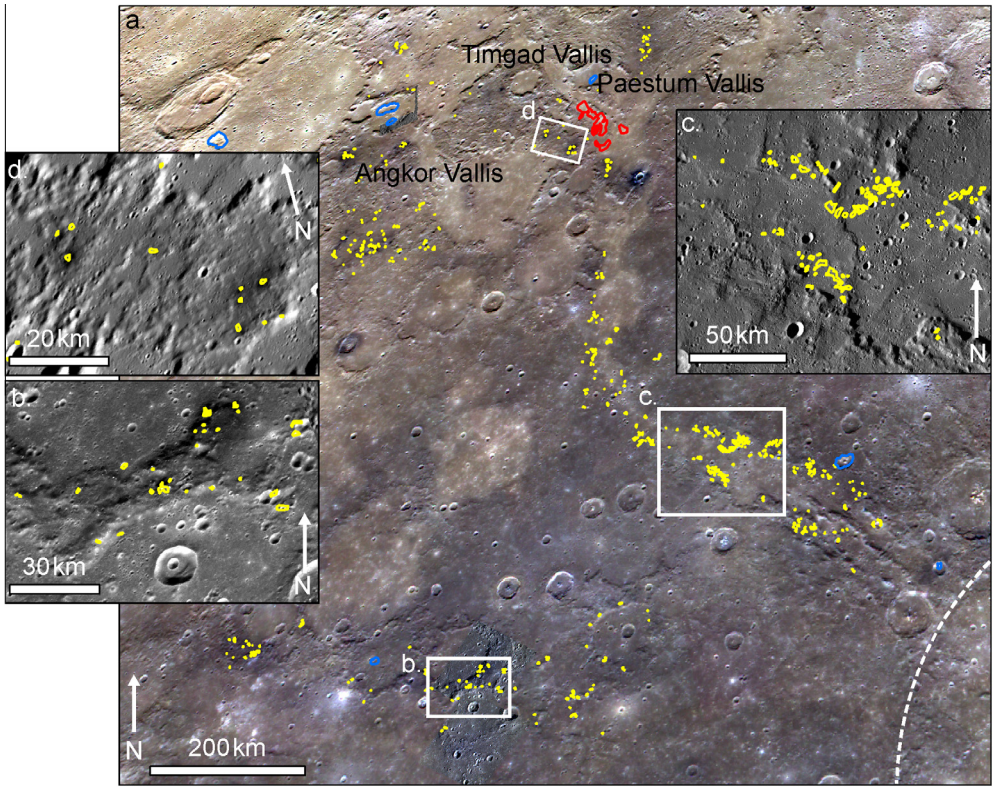


Fig. 9. (a) Two dispersed groupings of hollows (hollows outlined in yellow) occur to the northwest of the Caloris basin (dashed white line = basin rim). The northwest grouping extends to a region featuring several named valles, thought to be lava channels (Byrne et al., 2013), several pits (outlined in blue) and a group of areas of spectrally red pitted ground (outlined in red). Hollows associated with specific impact craters have been omitted from this diagram. Extent of insets indicated by white boxes (excerpt from the global colour mosaic); (b) hollow formation in the southern grouping occurs on LRM forming degraded crater rims (image ID EW0264188888G); (c) hollows in the mid-part of the northern grouping form at the margins and on the margin-proximal floor of a smooth, curvilinear unit of HRP (excerpt from the global monochrome mosaic); (d) hollows (outlined in yellow) occur in 'dark spots' on regions of the non-plains surface that are adjacent to smooth channel floors and appear superficially smoothed (mosaic of image ID EW0231135561G, EW0231135600G and EW0231135586G). (For interpretation of the references to colour in this figure legend, the reader is referred to the web version of this article.)

the northern smooth plains (Fig. 9c). In the far northwest, hollows preferentially form in and around localised very low reflectance deposits (dubbed 'dark spots' by Xiao et al. (2013)), which occur on a non-plains substrate adjacent to the smooth-floored channels and to pits that are possible sources of fluid lava that carved the channels (Byrne et al., 2013). The 'dark spots' occur on a rough, cratered substrate that appears superficially smoothed. This smoothing is particularly pronounced in lower elevation areas (Fig. 9d).

3.5. Association with pyroclastic features

Non-impact-related pits have hollows within 50 km of them in 74% of the cases where the resolution of the available images allows hollow identification, showing a strong association. 71% of these pits have surrounding spectrally-red deposits, proposed to be pyroclastic in origin (e.g. Kerber et al., 2011). The association between hollows and pits within craters is stronger than the association of hollows and pits outside craters. 77% of pits within craters have nearby hollows, while only 47% of pits outside craters do. All of the areas of spectrally red pitted ground that were imaged at a high-enough resolution to identify hollows did have hollows within 50 km of them.

The reverse relationship is not as strong: only 22% of hollow groups lie within 50 km of a pit or pitted spectrally red area, 93% of which have associated bright red deposits indicating pyroclastic activity. The areal extent of these groups of hollows is higher than average: they total 52.5% of the total hollowed area and have a mean extent per group of 307 km^2 (standard deviation = 855) (compared to a mean of 129 km^2 (standard deviation = 475) for the total population). Formation of hollows in the vicinity of pits is more frequent in longitude bins crossing the 'cold poles' than near the 'hot poles' (Fig. 10a), but variations in percentage of the hollowed area within those bins do not follow this pattern (Fig. 10b).

3.6. Association with regional substrates

Previous studies have indicated an association between hollow formation and low-reflectance material, both the regional LRM unit (Blewett et al., 2013) and localised, possibly lower reflectance (Xiao et al., 2013) deposits. The results of our survey support this: 96% of the total hollowed area occurs associated with either regional or localised low-reflectance material. The hollows incise the low-reflectance material and are floored and/or haloed by bright relatively blue material.

We found that hollows are considerably rarer on plains substrates: only ~7% of the hollowed area occurs on high-reflectance plains (HRP) and ~8% on low-reflectance blue plains (LBP). Where hollows occur on regional HRP, the low-reflectance material is almost always present at the surface locally (37 out of 38 cases). Local low-reflectance material is also present in 25 out of 33 cases where hollows occur on regional LBP.

The preference for hollow formation in low-reflectance material rather than high-reflectance plains is particularly clear where an impact crater straddles a contact between these two regional substrates: Fig. 11 shows an 80 km diameter crater that intersects the

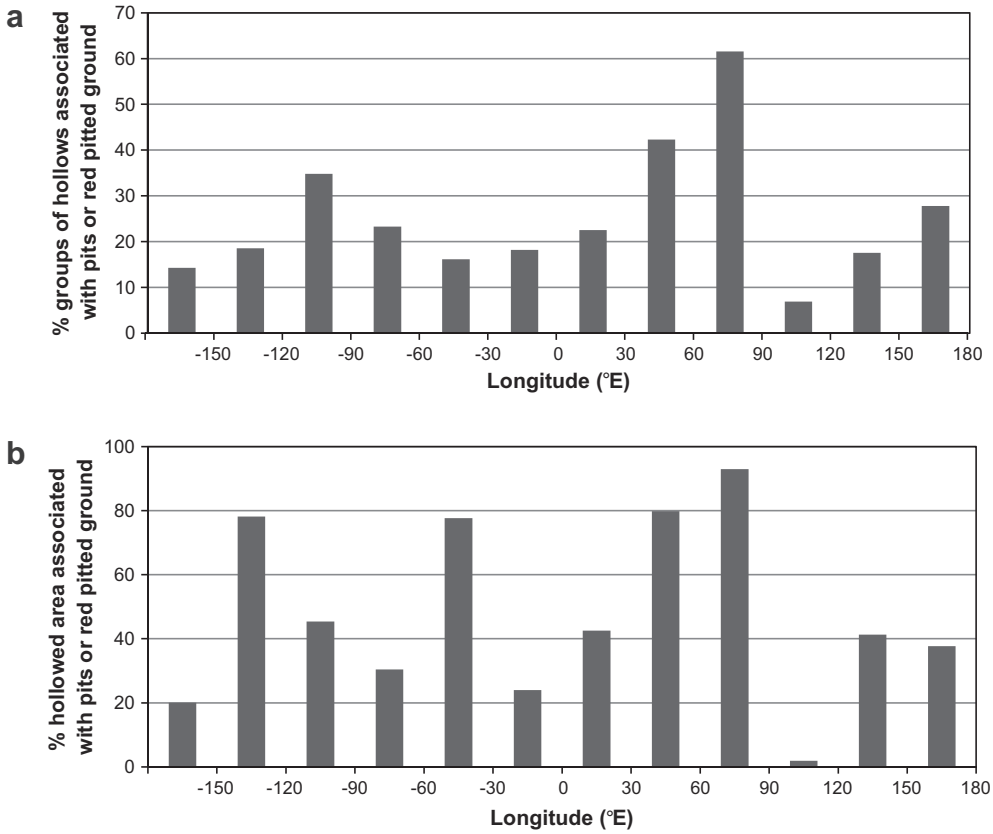


Fig. 10. Latitudinal variation in the association of hollows with pits and spectrally red pitted ground. (a) Hollows more commonly occur near these features at 'cold pole'-crossing latitudes (−90°E and 90°E) than at 'hot pole'-crossing latitudes (0°E and 180°E) but (b) the percentage of the surface area that is hollowed shows no regular variation.

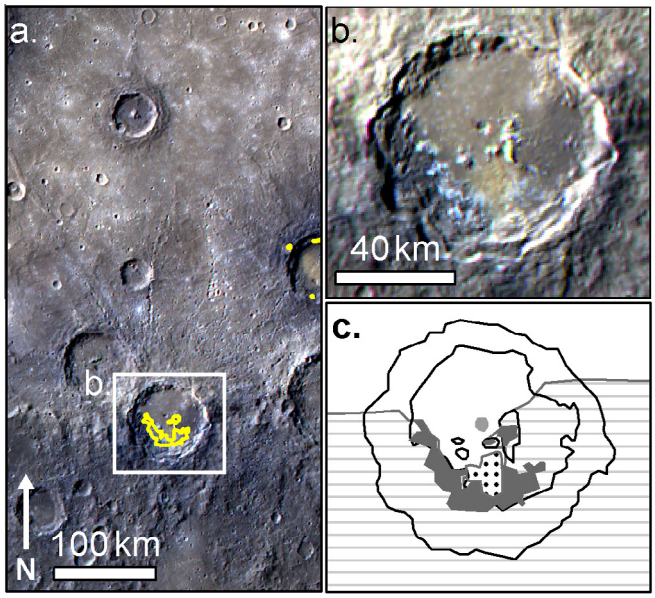


Fig. 11. Mansurian age crater straddling the southern rim of Rembrandt basin. Hollows (outlined in yellow) occur in the southern part of the crater, which has a low-reflectance substrate, and not in the high-reflectance northern part. (a) Location of the crater at the southern margin of Rembrandt basin (excerpt from global colour composite, centred at 88.1°E, −37.3°N); (b) the relation of hollows, a small pit and an pitted red area to the two substrates (colour composite based on EW0221673142G); (c) sketch map of the area in (b), black outlines: crater terraces and peak structures; dark grey: hollowed area; light grey: pit; dotted fill: pitted red area; hatched: LRM surfaces. (For interpretation of the references to colour in this figure legend, the reader is referred to the web version of this article.)

LRM rim of Rembrandt basin and its HRP fill. The north and south halves of the younger crater reflect the spectral properties of these substrates, and hollow formation is only seen in the low-reflectance substrate. This association supports the theory that the hollow-forming volatiles are derived from a constituent of low-reflectance material.

4. Discussion

The results presented in this study have implications for the mechanisms that form hollows and bring hollow-forming volatiles to the surface, and provide clues to the origin of these volatiles.

4.1. Hollow formation mechanisms

4.1.1. Exogenic processes

Previous studies have suggested that hollows may form by sublimation or by space weathering processes (Blewett et al., 2011), such as photon-stimulated desorption or sputtering by the solar wind.

Sublimation could form hollows if a moderately-volatile substance that is unstable at the temperatures and pressures at the surface of Mercury becomes exposed. It would then transition from solid to gas and be lost to space via the exosphere, leaving a depression. One reason why this is thought to be a viable mechanism is the morphological similarity between hollows and 'Swiss cheese' terrain in the south polar region of Mars. 'Swiss cheese' terrain is believed to form by scarp retreat as CO_2 ice sublimes (Byrne and Ingersoll, 2003a). The depth of sublimation may be limited by the thickness of the subliming layer: the CO_2 ice overlies a water

ice layer that is more stable. This may also apply for hollow formation, though unless the volatile component of hollow-forming material is 100%, accumulation of a residual lag is likely to limit hollow depth (Blewett et al., 2013).

'Swiss cheese' terrain is not a perfect analogue for hollows. The floors of the depressions in 'Swiss cheese' terrain are smooth and their outlines are more regular and cuspate. The cuspate outlines are believed to result from the consistency of the solar incidence angle through the day in polar regions (Thomas et al., 2000; Byrne and Ingersoll, 2003b). As most of the hollows we have observed are closer to the equator, it is perhaps not surprising that hollows have more irregular margins if sublimation is responsible for their formation. The uneven floors of hollows compared to Swiss cheese terrain suggest that unlike sublimation of CO_2 ice, the formation of hollows leaves an appreciable lag fraction, and is perhaps brought to a halt when the surface lag has reached a critical thickness.

If hollows form by sublimation, it is probable that their occurrence would be correlated with local and regional variations in insolation. Our results are consistent with this. Though few hollow groups show preferential formation on slopes of a particular orientation, when they do so there is a strong preference for the sun-facing slope (Fig. 5). The longitudinal variation in hollowing also supports a correlation with insolation intensity: when the effect of substrate is removed from a plot of the variation in the extent of hollowing at equatorial latitudes (Fig. 3b), it varies broadly with variations in the intensity of insolation. If surface temperature controls hollowing, one would expect to see a greater reduction in the extent of hollowing with increased latitude than at different longitudes because the difference in maximum surface temperature between the equator and poles is larger than between points on the equator (Peplowski et al., 2014). Our data show such a pattern, but observational biases and differences in substrate mean this is not a robust result.

Thus we find that hollow formation appears to be correlated with insolation intensity, but not strongly. In most cases hollows form on flat surfaces, or else hollows within a group occur on slopes with a variety of aspects. This may suggest that the threshold above which insolation causes hollow formation is commonly met on the surface of Mercury.

A correlation of hollow location with insolation intensity does not uniquely point to sublimation as the formation mechanism. High insolation also means a higher photon flux, promoting photon-stimulated desorption (PSD). In this process, UV photons strike the planetary surface and excite atoms, which are then desorbed and can be lost to the exosphere. This process is intensified by high temperatures, possibly due to enhanced diffusion to the topmost surface (Yakshinskiy and Madey, 2004), and PSD fluxes contributing to the exosphere are up to three times higher from equatorial surfaces at perihelion than at aphelion (Lammer et al., 2003). This is consistent with the disparity of our results at different equatorial longitudes. However, PSD is a phenomenon of the extreme surface, affecting the topmost layer of atoms. Unless the volatile elements that are susceptible to loss by this mechanism can be very efficiently delivered to the surface through any lag components, or unless churning of the regolith by impact gardening exposes fresh materials very efficiently, it is not probable that it plays a major part in hollow formation.

Another possibility is that hollow formation is enhanced by, rather than caused by, high daytime insolation, because this leads to greater diurnal temperature variation. The varying temperature in the top few tens of cm of the surface (Vasavada et al., 1999) could set up a circulation system that could concentrate volatiles sufficiently to allow hollow formation by one or more of the processes suggested here.

In light of the extreme conditions at Mercury, at an average of 0.387 AU from the Sun, the solar wind must be considered as a possible agent to produce hollows. When solar ions strike the planet's surface, they may remove material through momentum transfer in a process known as physical sputtering. The importance of this process is potentially testable by looking at latitudinal variations in hollow formation: under normal solar wind conditions, the maximum precipitation flux of solar wind ions onto Mercury's surface is expected at high latitudes due to their direction along open magnetic field lines (Sarantos et al., 2007), while other areas of the planet's surface are subject to ion bombardment only during relatively short-lived conditions of higher dynamic pressure (Siscoe and Christopher, 1975; Kabin et al., 2000; Slavin et al., 2010). This may mean the effects of physical sputtering are more pronounced at high latitudes than low latitudes. One would also expect a stronger effect on areas under the Sun at perihelion than at aphelion, as the flux through open field lines is modelled to vary by a factor of four and the area open to the solar wind by a factor of two between these orbital points (Sarantos et al., 2007). However, given the observational difficulties that hamper identification of hollows at polar and high southern latitudes and the presence of a plains substrate at high northern latitudes that appears to preclude hollow formation on compositional grounds, our current data does not allow us to confidently compare the extent of hollow formation at high vs. low latitudes. We do not rule out solar wind sputtering playing a part in hollow formation, though the stronger evidence for a correlation with insolation intensity at lower latitudes suggests that surface temperature plays a strong role and that sublimation is probably the dominant mechanism.

4.1.2. Endogenic processes

The strong correlation of pyroclastic pits and areas of spectrally red pitted ground with hollows (Section 3.5) suggests that endogenic heat sources may contribute to the heat necessary to release the volatiles within hollow-forming substrates. If magmatic activity was contemporaneous with hollow formation at these sites, the heat of subsurface magma may have mobilised the volatile component of the host rock. This component may either ascend to the surface, condense and later be removed by sublimation, possibly aided by heat from below, or ascend as a gas and cause hollows to form by collapse of surface material due to volume loss in the underlying substrate.

The first hypothesis best fits the evidence, as hollows around pits have the same morphology as those on crater surfaces. Though it is possible that hollows and pits are found together only because they both occur in the same substrates for independent reasons, it is revealing that the areal extent of hollowing is on average higher around pyroclastic pits than elsewhere. Additionally, at locations where there is less insolation and so initiation of hollows would be relatively more strongly affected by any endogenic component to volatile mobilisation, a higher proportion of hollow groups occur near pits. This suggests that proximity to pyroclastic pits leads to more hollow formation. Also, the percentage of the total hollowed area within each longitudinal band that is near pits is not strongly correlated to variations in the intensity of insolation (Fig. 10b), suggesting that conditions in the vicinity of particular pits exert a stronger control on the extent of hollowing than do variations in mean insolation.

The second hypothesis, that hollows form by surface collapse when hollow-forming volatiles are lost, may be a more suitable explanation for the shallow areas of pitted ground with red deposits. These areas look similar to hollows but are deeper, more uneven, have a less morphologically-crisp appearance and in all cases have hollows in their vicinity. They are also all found on smooth substrates, in most cases crater floors. This juxtaposition is seen clearly at Rachmaninoff basin (Fig. 12). Here, hollows form in the low-reflectance material of the crater's peak ring and walls, and on the younger volcanic crater fill (Marchi et al., 2011) around

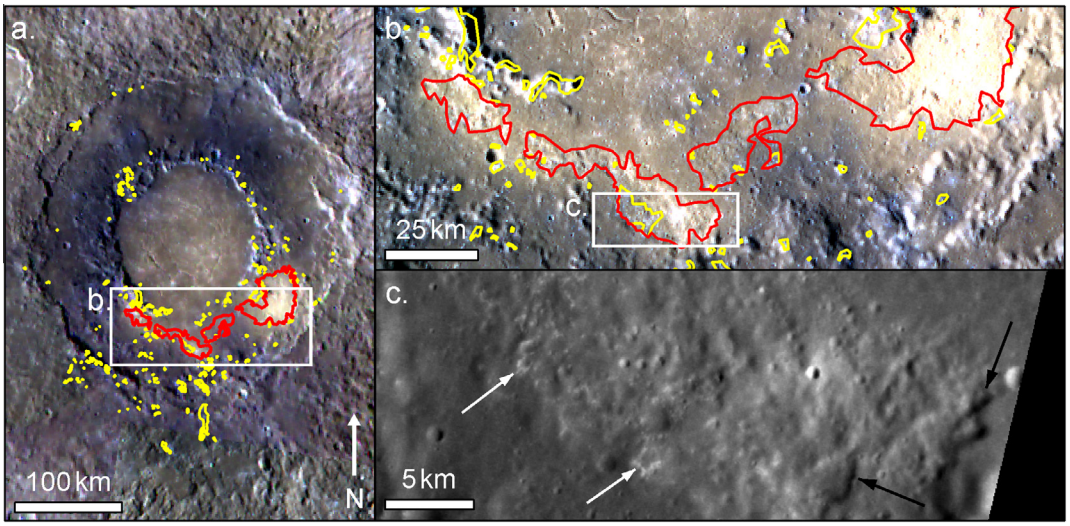


Fig. 12. (a) Hollows (outlined in yellow) form in low-reflectance material in the peak ring and walls of Rachmaninoff basin (3.6 Ga old (Marchi et al., 2011), 57.4°E, 27.6°N) and around bright, relatively-red areas (outlined in red) south of a breach in its peak ring (excerpt from global colour mosaic); (b) the area south of the breach in the peak ring, where the bright spectrally-red areas are seen to be areas of pitted ground with hollows near their margins (composite of EW0254942264G, EW0254942268F and EW0254942272I); (c) closeup of an area of pitted ground with steep margins at some points (black arrows) and hollow formation near its margins (white arrows) (EN0219350311M). (For interpretation of the references to colour in this figure legend, the reader is referred to the web version of this article.)

areas of spectrally red pitted ground. The presence of low-reflectance material on the crater's peak ring and walls suggests this material also forms the substrate to the volcanic infill. The lava may have heated the substrate and released its volatile component. Before the lava fully solidified, disruption of its surface by escaping volatiles and collapse due to volume loss in the substrate may have given it a pitted morphology. This can be seen as broadly analogous to the process by which pitted terrain is suggested to form by the release of volatiles through impact melt on Mars (Boyce et al., 2012) and Vesta (Denevi et al., 2012). The spectrally-red deposits may indicate that magmatic volatiles and entrained juvenile material also escaped to the surface along the same pathways as the hollow-forming volatiles.

Such a process may also explain the morphology of hollowed areas on crater floors over buried peaks rings, such as Sousa crater (Fig. 13). The morphology of these areas is similar to that of those areas of spectrally red pitted ground which lack margins, but they have no associated red deposits. Here the crater fill (either impact melt or a later volcanic infill) may have volatilised a component of the buried low-reflectance peak ring, and released this material to the surface at the point where the fill is thinnest. This led to collapse of the surface and some formation of crisper hollows where escaped material condensed on the surface before losing its volatile component via sublimation. This hypothesis is an extension of that of Blewett et al. (2013) that hollows may form through concentration of hollow-forming volatiles by contact heating.

The global distribution of hollows does not simply mirror variations in insolation, and many hollows occur at a distance from pits and potential pyroclastic activity and without contact with crater fills. A further factor plays a stronger controlling role on the formation of hollows: substrate. This determines the quantity of hollow-forming volatiles at and near the surface, and the ability of volatiles to ascend to the surface. We explore this aspect below.

4.2. Means of transfer of hollow-forming volatiles to the surface

4.2.1. Exhumation and exposure by impacts

The strong correlation of hollows with craters suggests a genetic link. The vast majority of hollows lie within impact craters and their proximal ejecta. Hollows do not form on volcanic plains except where these have been breached by later impacts, and most of the small hollow clusters that occur outside impact craters ap-

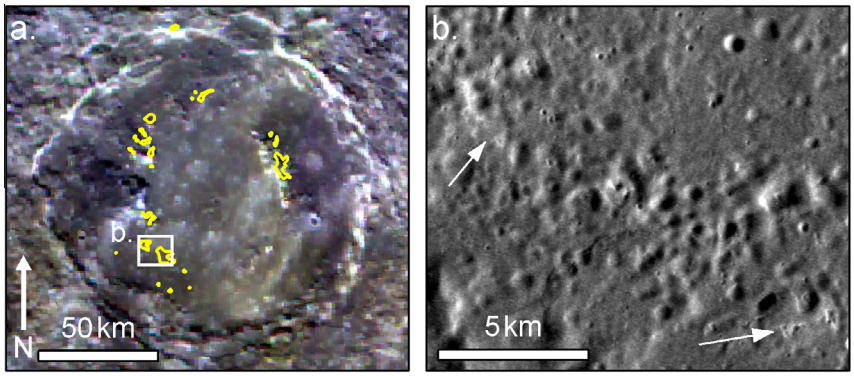


Fig. 13. Hollows (outlined in yellow) on the LRM peak ring and the crater fill where this overlies the peak ring in Sousa crater (Mansurian age, 0.5°E, 46.8°N). (a) Locations of hollows within the crater (outlined in yellow) (excerpt from global colour mosaic) and (b) close-up showing the majority of the hollowed region in the crater fill is pitted ground, with some small crisp hollows (white arrows) (mosaic of EN0251054159M and EN0251054171M). (For interpretation of the references to colour in this figure legend, the reader is referred to the web version of this article.)

pear to form in impact ejecta. For these reasons, it has previously been suggested that hollows form in material exposed and exhumed by large impacts (Blewett et al., 2011). Larger impacts sample the crust to great depths compared to smaller impacts, exposing the strata underlying the impacted surface in their walls and ejecta, and uplifting material from depth in their central structures. The evidence supports this as a mechanism for exposure of hollow-forming material. Hollows occur in low-reflectance material within impact craters, particularly on peak rings, which are the part of a crater that is exhumed from the greatest depth (Fig. 14). The surface distribution of this low-reflectance material is consistent with the substrate into which the crater incised (Fig. 11) as expected if it is exhumed material.

The lack of correlation between increasing crater age and extent of hollows (Fig. 7) could be seen as weakening this hypothesis: if hollowing begins at the time of crater formation, older craters should have a larger extent of hollows. However, firstly, the small scale of hollows means they may become obscured by later overlying ejecta over time and the areal extent of hollows visible in older craters may not be indicative of the true cumulative amount of hollow formation there. Secondly, if the quantity of material that can form hollows is limited, hollow formation would eventually cease. This explains the drop-off in observed hollowed extent in craters of Calorian age (degradation state 3) and older (Fig. 7).

Estimates of potential burial rates at Mercury's surface vary: regolith formation has been estimated at 5–10 m in the last 3–4 Ga (Langevin, 1997), while burial of polar ice deposits has been modelled to occur at a rate of 0.43 cm/Myr (Crider and Killen, 2005). The former rate would be sufficient to obscure the morphology of hollows and the latter to completely bury them in the estimated 3.9 Ga (Neukum et al., 2001)) since the Calorian period.

It has alternatively been suggested (Vaughan et al., 2012) that hollows form in material differentiated out of impact melt during crater formation. We find this to be an unconvincing explanation: hollows are found in small ejecta deposits distal from their host craters (Fig. 8) and on a variety of steep surfaces. While differentiation is viable in pooled melt, it is difficult to envision in settings such as these.

4.2.2. Post-impact exposure

The presence of hollows in even very old craters (Fig. 7) indicates that in these cases a process is operating that replenishes hollow-forming material at the surface of craters long after crater formation. Our observation that hollows in older craters are found in the walls of younger craters and on thrust faults (Fig. 6d) suggests that these are the agents of this late exposure. If hollow-forming material was exposed to surface conditions during the formation of the original crater, hollow formation may have ceased prior to its depletion in the near-surface due to deposition of a lag or burial by ejecta. Small new craters, crater-crossing thrust faults and fractures at fault-bend folds may have later exposed it to surface conditions, at which time fresh hollows formed.

Such processes may operate on a regional scale to produce the western broad area of distributed hollowing outside the Caloris basin (Fig. 9a). The low-reflectance deposits here are close enough to Caloris to have been deposited as ejecta from that impact, and may have originally been as volatile-rich as the extensively-hollowed, very dark LRM deposits that are exhumed by younger impacts into the Caloris fill. The heavily-cratered appearance of the hollowed surfaces suggests they are old and that any initial hollow formation in them would have long ceased, but smaller impacts and possibly mass wasting may continue to expose new volatile-bearing material to surface conditions and initiate new hollows.

The association of hollows with pyroclastic pits within craters could indicate that the structures associated with this volcanism aided the release of hollow-forming volatiles from depth. Pyroclastic pits occur primarily in parts of impact craters that are underlain by planes of weakness such as wall terraces and central structures. This suggests that crater-related faults act as conduits for the release of volatiles or volatile-bearing magma towards the surface, possibly aided by on-going fault movement in response to global contraction (Klimczak et al., 2013). The same may be true for hollow-forming volatiles. The evidence does not, however, allow a definite identification of this phenomenon. For example, Fig. 15 shows hollows around a pyroclastic pit in the north-west rim of a younger crater that intersects the wall of an older crater, and also hollows in small areas to its south. This could be explained by the migration of hollow-forming volatiles up the same crater-wall faults as were exploited by the probable pyroclastic volcanism. However, exhumation is a viable alternative explanation: hollow-forming volatiles may have been present in the deeply-excavated wall material of the older crater and then been exposed by the younger crater. The small cluster of distal hollows may be located in the ejecta from this impact. In this scenario, the association of hollows with pyroclastic volcanism may be partly due to the spatial coincidence of deep fractures that are conducive to magma ascent with volatile-bearing wall rocks, and possibly, if hollow formation and volcanism were contemporaneous, partly due to increased heat flow in this area enhancing upward diffusion of volatiles or hollow formation by sublimation (Section 4.1).

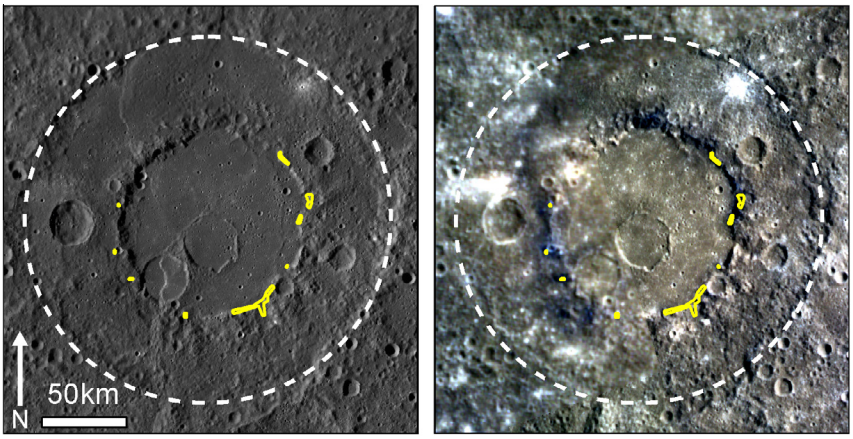


Fig. 14. Localisation of hollows (outlined in yellow) and low-reflectance deposits in the peak ring of Renoir basin (Tolstojan age, −51.8°E, −18.3°N). Dashed white line shows the outer rim of the basin, where no low-reflectance material or hollows are observed. Left: excerpt from global monochrome mosaic; right: mosaic of colour composites based on EW0253851174G, EW0253851412G and EW0241374406G. (For interpretation of the references to colour in this figure legend, the reader is referred to the web version of this article.)

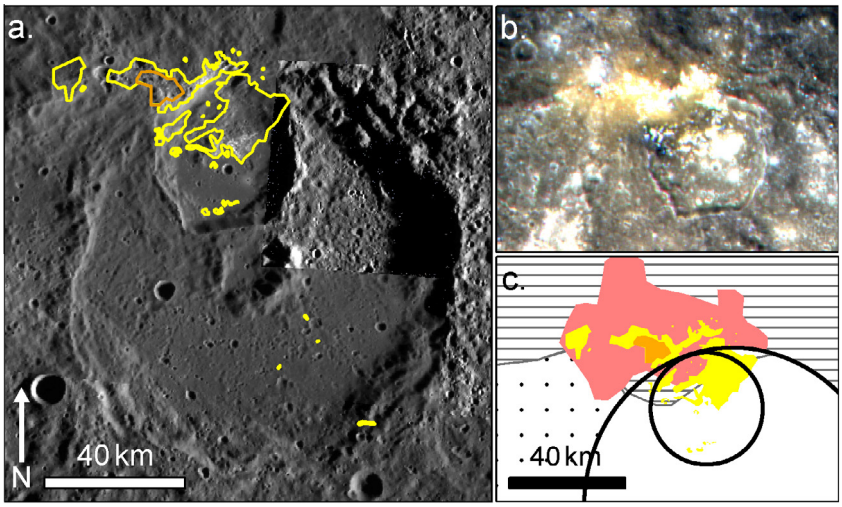


Fig. 15. (a) Hollows (outlined in yellow) occur at the north-west edge of a Calorian age crater at −3.6°E, 25.6°N, around a pyroclastic pit (outlined in orange) and scattered towards the south. This may be due to explosive escape of hollow-forming volatiles up the same conduits as used by the pyroclastic volcanism, or, if the two phenomena were contemporaneous, hollow formation in crater deposits and ejecta intensified in the region of volcanism by endogenic heat flow (MESSENGER global monochrome mosaic); (b) colour composite of the superposed crater in the north (based on EW0225312562G); (c) sketch map of (b), hatched area: low-reflectance material; dotted area: bright ejecta; pink area: bright 'red' deposits; orange area: pit; yellow area: hollowed area; black outline: crater walls. (For interpretation of the references to colour in this figure legend, the reader is referred to the web version of this article.)

4.2.3. Exposure outside craters

A non-impact-related process is necessary to explain the exposure of hollow-forming material to produce the broad area of distributed hollowing along a curvilinear unit of HRP to the northwest of Caloris. These hollows form in LBP and on LRM outcrops standing above the plains. We propose that the HRP unit is a lava flow, and that contact heating by this material caused concentration of volatiles from within the LBP and LRM substrates at the surface (in a process similar to that suggested for other incidences of hollowing by Blewett et al. (2013)), after which hollows formed by sublimation.

The formation of hollows in small 'dark spots' at the far northwest of this grouping (Fig. 9d) is more enigmatic. These 'dark spots' occur on a non-plains substrate in which lower elevation areas appear anomalously smooth, adjacent to broad, smooth-floored channels and to the pits that have been suggested as the source of voluminous lavas that carved those channels (Byrne et al., 2012; Hurwitz et al., 2013). It is possible that the surface here appears somewhat smoothed because it has been draped by a thin layer of lava. This may have covered a volatile-bearing substrate to a shallow depth. Subsequently either a high regional heatflow connected to magmatic activity volatilised the underlying substrate or burial was sufficiently shallow (<1 m (Vasavada et al., 1999)) for penetration of solar heating do so. Pressure built up and finally volatiles were released through fractures in the overlying material. This is consistent with the hypothesis that 'dark spots' form during intense outgassing during hollow formation (Xiao et al., 2013). This process may have directly produced hollows in the manner of fumerolic vents, or through deposition of the volatile-rich dark material on the surface followed by its sublimation.

4.3. Nature of the hollow-forming material

Hollows are commonly found in low-reflectance material. Conversely, they are found in high-reflectance smooth plains only where low-reflectance material is locally present such as where younger impact craters exhume it from beneath the volcanic fill of the Caloris basin.

This strongly suggests that the volatile material responsible for hollow formation is not present in high-reflectance flood lavas, but is a component of low-reflectance material. The nature of low-reflectance deposits on Mercury is not yet established, although it has been suggested that the regional LRM unit could be primary crust (Rothery et al., 2010) or a cumulate darkened by Fe- or Ti-bearing or other opaque oxides (Denevi et al., 2009; Riner et al., 2009). Space weathering complicates the determination of the composition of LRM on the basis of reflectance: the creation of nanophase iron during space weathering leads to more darkening of rock types initially richer in iron, so the albedo of any rock is the product of its composition and mineralogy, its exposure time and its susceptibility to space weathering (Riner and Lucey, 2012).

The presence of low-reflectance material in some craters of a particular diameter (and thus excavation depth) and absence in others shows that low-reflectance material is not present globally at a specific depth, so variations in the igneous and/or tectonic history of different parts of Mercury's crust appear to play a role in its occurrence. For example, the formation of the Caloris impact basin may have exhumed large amounts of this material, providing the substrate for the broad regions of dispersed hollow formation to its northwest.

The relatively lower reflectance of some localised deposits around hollows (Xiao et al., 2013) may suggest that before LRM has been hollowed it contains an additional darkening agent, and that this is the hollow-forming volatile. This may explain the presence of bright material in haloes around hollows and on their floors, which could be a brighter residue formed by the removal of a spectrally dark component (Blewett et al., 2013). Alternatively, the high reflectivity of these deposits may be due to an unusual texture or small grain size (Blewett et al., 2013). The diffused margins of the haloes suggest two possible emplacement mechanisms for the bright material: (a) ballistic ejection of a bright component as a result of high-energy escape of the hollow-forming volatiles, or (b) diffusive alteration of hollow wall rock as a result of chemical reactions during hollow formation. In both cases, either the compositional or physical characteristics of these bright deposits could potentially be the cause of their high reflectance.

The composition of the darker, volatile component is as yet unknown, but will perhaps be resolved when BepiColombo with its higher-resolution visible-NIR, thermal infrared and X-ray spectrometers (Rothery et al., 2010) arrives at Mercury in the coming decade.

5. Conclusions

1. In a global survey of the surface of Mercury, we found that the shallow rimless depressions known as hollows cover ~57,400 km^2, which is 0.08% of the total surface imaged at better than 180 m/px.
2. A weak overall correlation was found between hollow occurrence and insolation, as well as a possible correlation with subsurface heat sources. Both suggest a thermal control on hollow formation, thus supporting sublimation as the primary hollow-forming mechanism.
3. In most cases it appears probable that material containing hollow-forming volatiles was exposed and exhumed from depth by large impacts.
4. Some small impact craters and thrust faults within older craters also have hollows, hence these structures may expose subsurface hollow-forming material or facilitate the migration of volatiles to the surface. This suggests that some volatiles remain in the near-subsurface even after hollow formation has ceased at the surface.
5. Hollows do not occur in volcanic plains but are found mostly in low-reflectance material. This suggests that this low-reflectance material has a volatile component, and that hollows are formed by loss of that component. The widespread occurrence of hollows suggests that this material is similarly widespread within the crust of Mercury.

Acknowledgments

Rebecca Thomas acknowledges support via a PhD grant from the Science and Technology Facilities Council (UK) and David Rothery acknowledges support from the UK Space Agency in preparation for the BepiColombo mission. Excerpts from global mosaics used in figures in this paper are credited to NASA/Johns Hopkins University Applied Physics Laboratory/Carnegie Institution of Washington, and the NAC and WAC images are credited to NASA/JPL-Caltech. We thank David Blewett and Laura Kerber for their constructive and insightful reviews that helped improve the quality of the manuscript. We also thank Oded Aharonson for his editorial handling.

Appendix A. Supplementary material

Supplementary data associated with this article can be found, in the online version, at http://dx.doi.org/10.1016/j.icarus.2013.11.018.

References

Barnouin, O.S., Zuber, M.T., Smith, D.E., Neumann, G.a., Herrick, R.R., Chappelow, J.E., Murchie, S.L., Prockter, L.M., 2012. The morphology of craters on Mercury: Results from MESSENGER flybys. Icarus 219 (1), 414–427. http://dx.doi.org/10.1016/j.icarus.2012.02.029.

Blewett, D.T. et al., 2009. Multispectral images of Mercury from the first MESSENGER flyby: Analysis of global and regional color trends. Earth Planet. Sci. Lett. 285 (3–4), 272–282. http://dx.doi.org/10.1016/j.epsl.2009.02.021.

Blewett, D.T. et al., 2011. Hollows on Mercury: MESSENGER evidence for geologically recent volatile-related activity. Science 333 (6051), 1856–1859. http://dx.doi.org/10.1126/science.1211681.

Blewett, D.T. et al., 2013. Mercury's hollows: Constraints on formation and composition from analysis of geological setting and spectral reflectance. J. Geophys. Res. – Planets 118 (5), 1013–1032.

Boyce, J.M., Wilson, L., Mouginis-Mark, P.J., Hamilton, C.W., Tornabene, L.L., 2012. Origin of small pits in martian impact craters. Icarus 221 (1), 262–275. http://dx.doi.org/10.1016/j.icarus.2012.07.027.

Byrne, S., Ingersoll, AP., 2003a. A sublimation model for martian south polar ice features. Science 299 (5609), 1051–1053. http://dx.doi.org/10.1126/science.1080148.

Byrne, S., Ingersoll, A.P., 2003b. Martian climatic events on timescales of centuries: Evidence from feature morphology in the residual south polar ice cap. Geophys. Res. Lett. 30 (13), 2–5. http://dx.doi.org/10.1029/2003GL017597.

Byrne, P.K. et al., 2012. An assemblage of lava flow features on Mercury. J. Geophys. Res. – Planets. http://dx.doi.org/10.1002/JGRE.20052.

Byrne, P.K. et al., 2013. An assemblage of lava flow features on Mercury. J. Geophys. Res. – Planets 118 (6), 1303–1322. http://dx.doi.org/10.1002/jgre.20052.

Chabot, N.L. et al., 2013. Craters hosting radar-bright deposits in Mercury's north polar region: Areas of persistent shadow determined from MESSENGER images. J. Geophys. Res. – Planets 118 (1), 26–36. http://dx.doi.org/10.1029/2012JE004172.

Cheng, A.F., Johnson, R.E., Krimigis, S.M., Lanzerotti, L.J., 1987. Magnetosphere, exosphere, and surface of Mercury. Icarus 71, 430–440. http://dx.doi.org/10.1016/0019-1035(87)90038-8.

Crider, D., Killen, R.M., 2005. Burial rate of Mercury's polar volatile deposits. Geophys. Res. Lett. 32 (12), L12201. http://dx.doi.org/10.1029/2005GL022689.

Denevi, BW. et al., 2009. The evolution of Mercury's crust: A global perspective from MESSENGER. Science 324 (5927), 613–618. http://dx.doi.org/10.1126/science.1172226.

Denevi, B.W. et al., 2012. Pitted terrain on Vesta and implications for the presence of volatiles. Science 338 (6104), 246–249. http://dx.doi.org/10.1126/science.1225374.

Denevi, B.W. et al., 2013. The distribution and origin of smooth plains on Mercury. J. Geophys. Res. – Planets 118 (5), 891–907. http://dx.doi.org/10.1002/jgre.20075.

Dzurisin, D., 1977. Mercurian bright patches: Evidence for physio-chemical alteration of surface material? Geophys. Res. Lett. 4 (10), 383–386.

Evans, L.G. et al., 2012. Major-element abundances on the surface of Mercury: Results from the MESSENGER Gamma-Ray Spectrometer. J. Geophys. Res. 117, E00L07. http://dx.doi.org/10.1029/2012JE004178.

Fassett, C.I. et al., 2009. Caloris impact basin: Exterior geomorphology, stratigraphy, morphometry, radial sculpture, and smooth plains deposits. Earth Planet. Sci. Lett. 285 (3–4), 297–308. http://dx.doi.org/10.1016/j.epsl.2009.05.022.

Gillis-Davis, J.J. et al., 2009. Pit-floor craters on Mercury: Evidence of near-surface igneous activity. Earth Planet. Sci. Lett. 285 (3–4), 243–250. http://dx.doi.org/10.1016/j.epsl.2009.05.023.

Goldsten, J.O. et al., 2007. The MESSENGER Gamma-Ray and Neutron Spectrometer. Space Sci. Rev. 131 (1–4), 339–391. http://dx.doi.org/10.1007/s11214-007-9262-7.

Hawkins, S.E. et al., 2007. The Mercury Dual Imaging System on the MESSENGER Spacecraft. Space Sci. Rev. 131 (1–4), 247–338. http://dx.doi.org/10.1007/s11214-007-9266-3.

Hawkins, S.E. et al., 2009. In-flight performance of MESSENGER's Mercury Dual Imaging System. Proc. SPIE Int. Soc. Opt. Eng. SPIE7441. http://dx.doi.org/10.1117/12.826370.

Helbert, J., Maturilli, A., D'Amore, M., 2013. Visible and near-infrared reflectance spectra of thermally processed synthetic sulfides as a potential analog for the hollow forming materials on Mercury. Earth Planet. Sci. Lett. 369–370, 233–238. http://dx.doi.org/10.1016/j.epsl.2013.03.045.

Herrick, R.R., Curran, L.L., Baer, A.T., 2011. A Mariner/MESSENGER global catalog of mercurian craters. Icarus 215 (1), 452–454. http://dx.doi.org/10.1016/j.icarus.2011.06.021.

Hurwitz, D.M. et al., 2013. Investigating the origin of candidate lava channels on Mercury with MESSENGER data: Theory and observations. J. Geophys. Res. – Planets 118 (3), 471–486. http://dx.doi.org/10.1029/2012JE004103.

Jenness, J., 2011. Tools for graphics and shapes: extension for ArcGIS. Jenness Enterp.

Kabin, K., Gombosi, T.I., Dezeeuw, D.L., Powell, K.G., 2000. Interaction of Mercury with the solar wind. Icarus 143 (2), 397–406. http://dx.doi.org/10.1006/icar.1999.6252.

Kerber, L., Head, J.W., Solomon, S.C., Murchie, S.L., Blewett, D.T., Wilson, L., 2009. Explosive volcanic eruptions on Mercury: Eruption conditions, magma volatile content, and implications for interior volatile abundances. Earth Planet. Sci. Lett. 285 (3–4), 263–271. http://dx.doi.org/10.1016/j.epsl.2009.04.037.

Kerber, L. et al., 2011. The global distribution of pyroclastic deposits on Mercury: The view from MESSENGER flybys 1–3. Planet. Space Sci. 59 (15), 1895–1909. http://dx.doi.org/10.1016/j.pss.2011.03.020.

Killen, R.M., Sarantos, M., Reiff, P.H., 2004. Space weather at Mercury. Adv. Space Res. 33 (11), 1899–1904. http://dx.doi.org/10.1016/j.asr.2003.02.020.

Killen, R. et al., 2007. Processes that promote and deplete the exosphere of Mercury. Space Sci. Rev. 132 (2–4), 433–509. http://dx.doi.org/10.1007/s11214-007-9232-0.

Klimczak, C. et al., 2013. The role of thrust faults as conduits for volatiles on Mercury. Lunar Planet. Sci. 44. Abstract 1390.

Lammer, H., Wurz, P., Patel, M.R., Killen, R., Kolb, C., Massetti, S., Orsini, S., Milillo, A., 2003. The variability of Mercury's exosphere by particle and radiation induced surface release processes. Icarus 166 (2), 238–247. http://dx.doi.org/10.1016/j.icarus.2003.08.012.

Langevin, Y., 1997. The regolith of Mercury: Present knowledge and implications for the Mercury Orbiter mission. Planet. Space Sci. 45 (1), 31–37.

Madey, T.E., Yakshinskiy, BV., Ageev, V.N., Johnson, RE., 1998. Desorption of alkali atoms and ions from oxide surfaces: Relevance to origins of Na and K in atmospheres of Mercury and the Moon. J. Geophys. Res. 103 (E3), 5873–5887.

Marchi, S., Massironi, M., Cremonese, G., Martellato, E., Giacomini, L., Prockter, L., 2011. The effects of the target material properties and layering on the crater chronology: The case of Raditladi and Rachmaninoff basins on Mercury. Planet. Space Sci. 59 (15), 1968–1980. http://dx.doi.org/10.1016/j.pss.2011.06.007.

Melosh, H.J., McKinnon, W.B., 1988. The tectonics of Mercury. Mercury, 374–400.
Mura, A., Wurz, P., Lichtenegger, H.I.M., Schleicher, H., Lammer, H., Delcourt, D., Milillo, A., Orsini, S., Massetti, S., Khodachenko, M.L., 2009. The sodium exosphere of Mercury: Comparison between observations during Mercury's transit and model results. Icarus 200 (1), 1–11. http://dx.doi.org/10.1016/j.icarus.2008.11.014.
Neukum, G., Oberst, J., Ho, H., Wagner, R., Ivanov, B.A., 2001. Geologic evolution and cratering history of Mercury. Planet. Space Sci. 49, 1507–1521.
Nittler, LR. et al., 2011. The major-element composition of Mercury's surface from MESSENGER X-ray spectrometry. Science 333 (6051), 1847–1850. http://dx.doi.org/10.1126/science.1211567.
Peplowski, P.N. et al., 2011. Radioactive elements on Mercury's surface from MESSENGER: Implications for the planet's formation and evolution. Science 333, 1850–1852. http://dx.doi.org/10.1126/science.1211576.
Peplowski, P.N. et al., 2014. Enhanced sodium abundance in Mercury's north polar region revealed by the MESSENGER Gamma-Ray Spectrometer. Icarus 228, 86–95.
Potter, A.E., 1995. Chemical sputtering could produce sodium vapor and ice on Mercury. Geophys. Res. Lett. 22 (23), 3289–3292.
Riner, M.a., Lucey, P.G., 2012. Spectral effects of space weathering on Mercury: The role of composition and environment. Geophys. Res. Lett. 39, L12201. http://dx.doi.org/10.1029/2012GL052065.
Riner, M.a., Lucey, P.G., Desch, S.J., McCubbin, F.M., 2009. Nature of opaque components on Mercury: Insights into a mercurian magma ocean. Geophys. Res. Lett. 36 (L02201). http://dx.doi.org/10.1029/2008GL036128.
Robinson, M.S. et al., 2008. Reflectance and color variations on Mercury: Regolith processes and compositional heterogeneity. Science 321 (5885), 66–69. http://dx.doi.org/10.1126/science.1160080.
Rothery, D. et al., 2010. Mercury's surface and composition to be studied by BepiColombo. Planet. Space Sci. 58 (1–2), 21–39. http://dx.doi.org/10.1016/j.pss.2008.09.001.
Rothery, D.A., Thomas, R.J., Kerber, L., 2014. Prolonged eruptive history of a compound volcano on Mercury: Volcanic and tectonic implications. Earth Planet. Sci. Lett. 385, 59–67.
Sarantos, M., Killen, R.M., Kim, D., 2007. Predicting the long-term solar wind ion-sputtering source at Mercury. Planet. Space Sci. 55 (11), 1584–1595. http://dx.doi.org/10.1016/j.pss.2006.10.011.
Schlemm, C.E. et al., 2007. The X-ray spectrometer on the MESSENGER Spacecraft. Space Sci. Rev. 131 (1–4), 393–415. http://dx.doi.org/10.1007/s11214-007-9248-5.
Siscoe, G., Christopher, L., 1975. Variations in the solar wind stand-off distance at Mercury. Geophys. Res. Lett. 2 (4), 158–160.
Slavin, J.a. et al., 2010. MESSENGER observations of extreme loading and unloading of Mercury's magnetic tail. Science 329 (5992), 665–668. http://dx.doi.org/10.1126/science.1188067.
Strom, R.G., Trask, N.J., Guest, J.E., 1975. Tectonism and volcanism on Mercury. J. Geophys. Res. 80 (17), 2478–2507. http://dx.doi.org/10.1029/JB080i017p02478.
Thomas, PC. et al., 2000. North–south geological differences between the residual polar caps on Mars. Nature 404 (6774), 161–164. http://dx.doi.org/10.1038/35004528.
Vasavada, A.R., Paige, D.A., Wood, S.E., 1999. Near-surface temperatures on Mercury and the Moon and the stability of polar ice deposits 1. Icarus 141, 179–193.
Vaughan, W.M. et al., 2012. Hollow-forming layers in impact craters on Mercury: Massive sulfide or chloride deposits formed by impact melt differentiation? Lunar Planet. Sci. 43, 1187.
Watters, T.R. et al., 2009. The tectonics of Mercury: The view after MESSENGER's first flyby. Earth Planet. Sci. Lett. 285 (3–4), 283–296. http://dx.doi.org/10.1016/j.epsl.2009.01.025.
Weider, S.Z. et al., 2012. Chemical heterogeneity on Mercury's surface revealed by the MESSENGER X-Ray Spectrometer. J. Geophys. Res. 117, 1–15. http://dx.doi.org/10.1029/2012JE004153.
Xiao, Z. et al., 2013. Dark spots on Mercury: A distinctive low-reflectance material and its relation to hollows. J. Geophys. Res. – Planets 118, 1–14. http://dx.doi.org/10.1002/jgre.20115.
Yakshinskiy, B.V., Madey, T.E., 2004. Photon-stimulated desorption of Na from a lunar sample: Temperature-dependent effects. Icarus 168 (1), 53–59. http://dx.doi.org/10.1016/j.icarus.2003.12.007.